Formation of Ti–Zr–Cu–Ni bulk metallic glasses

X. H. Lin[a] and W. L. Johnson
W. M. Keck Laboratory of Engineering Materials, California Institute of Technology, Pasadena, California 91125

(Received 30 May 1995; accepted for publication 17 August 1995)

Formation of bulk metallic glass in quaternary Ti–Zr–Cu–Ni alloys by relatively slow cooling from the melt is reported. Thick strips of metallic glass were obtained by the method of metal mold casting. The glass forming ability of the quaternary alloys exceeds that of binary or ternary alloys containing the same elements due to the complexity of the system. The best glass forming alloys such as $Ti_{34}Zr_{11}Cu_{47}Ni_8$ can be cast to at least 4-mm-thick amorphous strips. The critical cooling rate for glass formation is of the order of 250 K/s or less, at least two orders of magnitude lower than that of the best ternary alloys. The glass transition, crystallization, and melting behavior of the alloys were studied by differential scanning calorimetry. The amorphous alloys exhibit a significant undercooled liquid region between the glass transition and first crystallization event. The glass forming ability of these alloys, as determined by the critical cooling rate, exceeds what is expected based on the reduced glass transition temperature. It is also found that the glass forming ability for alloys of similar reduced glass transition temperature can differ by two orders of magnitude as defined by critical cooling rates. The origins of the difference in glass forming ability of the alloys are discussed. It is found that when large composition redistribution accompanies crystallization, glass formation is enhanced. The excellent glass forming ability of alloys such as $Ti_{34}Zr_{11}Cu_{47}Ni_8$ is a result of simultaneously minimizing the nucleation rate of the competing crystalline phases. The ternary/quaternary Laves phase ($MgZn_2$ type) shows the greatest ease of nucleation and plays a key role in determining the optimum compositions for glass formation.

I. INTRODUCTION

The reduced glass transition temperature T_{rg} of glass forming alloys, which is the ratio of glass transition temperature T_g to melting temperature T_m, plays an important role in determining the glass forming ability of alloys.[1,2] Alloys having higher T_{rg} generally exhibit better glass forming ability (GFA). The critical cooling rate required to avoid the formation of detectable fraction of crystal in quenching molten alloys is used in describing the glass forming ability of materials. In quenching molten alloys, a sample of typical dimension R and initial temperature T_m will require a total cooling time τ (to T_g) of the order of:

$$\tau \sim (R^2/\kappa), \tag{1}$$

where κ is the thermal diffusivity of the alloy. It is given by $\kappa = K/C$ where K is the thermal conductivity and C is the heat capacity per unit volume. The cooling rate achieved will be of the order of

$$\dot{T} = \frac{dT}{dt} = \frac{(T_m - T_g)}{\tau} = \frac{K(T_m - T_g)}{CR^2}. \tag{2}$$

Taking $T_m - T_g \sim 400$ K, $K \sim 0.1$ W/cm s^{-1} K^{-1} (typical of a molten alloys), and $C \sim 4$ J/cm^3 K^{-1} (also typical of molten alloys), gives

$$\dot{T}(\mathrm{K/s}) = 10/R^2(\mathrm{cm}). \tag{3}$$

Therefore, the maximum thickness of the amorphous alloy is determined by the critical cooling rate of the material. Notice that one order of magnitude increasing in the maximum dimension is equivalent to a two order of magnitude decrease in the critical cooling rate. Figure 1 shows the critical cooling rates for a number of glass forming alloys as a function of the reduced glass transition temperature and corresponding maximum dimension. The values of alloys 1–17 in this figure are taken from Davies.[3] The critical cooling rate for $Zr_{41.2}Ti_{13.8}Cu_{12.5}Ni_{10}Be_{22.5}$ (Ref. 4) is taken from direct measurement by using an electrostatic levitation facility.[5] The critical cooling rates of other alloys are the upper limit values estimated by taking the value of the maximum thickness of an amorphous ribbon obtained by melt spinning or half the value of the reported maximum dimension for glass phases obtained by normal metal mold casting as maximum thickness, and by assuming ideal cooling. The actual critical cooling rates may be lower.

In many alloy systems T_g does not vary with composition as rapidly as T_m. Therefore, it is frequently the case that alloys near deep eutectics have high T_{rg} and, hence, exhibit better glass forming ability. The Ti–Cu, Zr–Cu, Ti–Ni, and Zr–Ni systems all exhibit deep eutectics. Binary alloys in these systems have been known to form glass by rapid solidification for many years. On the other hand, the crystal structures of the binary intermetallic compounds which form in these binary alloys differ among the systems. Thus, one expects to find ternary or quaternary eutectics in the Ti–Zr–Cu–Ni system, and the quaternary eutectic melting temperatures may be lower than those of the binary systems. As such, alloys near the quaternary eutectics may show greater glass forming ability than corresponding binary alloys.

[a]Electronic mail: xhlin@cco.caltech.edu

 0021-8979/95/78(11)/6514/6/$6.00

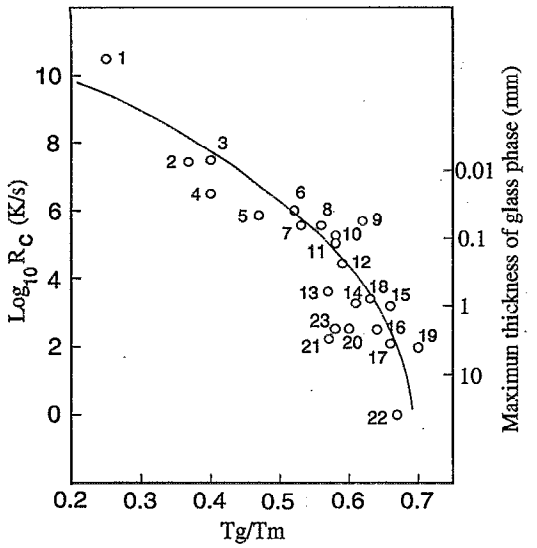

FIG. 1. Critical cooling rates for glass formation and corresponding maximum thickness of glass phase. Key to the alloys: (1) Ni; (2) $Fe_{91}B_9$; (3) $Fe_{89}B_{11}$; (4) Te; (5) $Au_{77.8}Ge_{13.8}Si_{8.4}$; (6) $Fe_{83}B_{17}$; (7) $Fe_{41.5}Ni_{41.5}B_{17}$; (8) $Co_{75}Si_{15}B_{10}$; (9) Ge; (10) $Fe_{79}Si_{10}B_{11}$; (11) $Ni_{75}Si_8B_{17}$; (12) $Fe_{80}P_{13}C_7$; (13) $Pt_{60}Ni_{15}P_{25}$; (14) $Pd_{82}Si_{18}$; (15) $Ni_{62.4}Nb_{37.6}$; (16) $Pd_{77.5}Cu_6Si_{16.5}$; (17) $Pd_{40}Ni_{40}P_{20}$ (above from Ref. 3); (18) $Au_{55}Pb_{22.5}Sb_{22.5}$ (Ref. 6); (19) $La_{55}Al_{25}Ni_{10}Cu_{10}$ (Ref. 7); (20) $Mg_{65}Cu_{25}Y_{10}$ (Ref. 8); (21) $Zr_{65}Cu_{17.5}Ni_{10}Al_{7.5}$ (Ref. 9); (22) $Zr_{41.2}Ti_{13.8}Cu_{12.5}Ni_{10}Be_{22.5}$ (Refs. 4 and 5); (23) $Ti_{34}Zr_{11}Cu_{47}Ni_8$.

The phase diagrams of ternary Ti–Zr–Ni and Ti–Zr–Cu have been studied respectively by two different groups. For the Ti–Zr–Ni system,[10] it was found that for the phase diagram section of Ti_2Ni–Zr_2Ni, replacing Ti with Zr up to 13.5 at. % in Ti_2Ni leads to a lowering of liquidus temperature from 1273 to 1173 K. Replacing Zr with Ti in Zr_2Ni up to 22.7 at. % Ti leads to a lowering of liquidus temperature from 1313 to 1123 K (the melting temperature of Zr_2Ni used here is different from the 1393 K value given in the binary alloy phase diagrams[11]). From 13.5 to 44 at. % of Zr, the liquidus temperature rises to 1193 K owing to the appearance of a new ternary "$MgZn_2$-type" Laves phase. For Ti–Zr–Cu system,[12] near the section of TiCu–ZrCu, three eutectics were found at $Ti_{34.42}Zr_{17.98}Cu_{47.59}$, $Ti_{14.24}Zr_{37.13}Cu_{48.63}$, and $Ti_{17.37}Zr_{43.20}Cu_{39.43}$. Between these three eutectics, there is also a ternary $MgZn_2$-type Laves phase. Massalski, Woychik, and Dutkiewicz have reported a very broad glass forming region for ternary Ti–Zr–Cu alloys by melt spinning.[13] The thickness of the melt-spun ribbons is about 50 μm, and the estimated cooling rate is about 5×10^5 K/s.

We have used a copper mold-casting technique to examine the glass forming ability of both Ti–Zr–Ni and Ti–Zr–Cu alloys. We found no Ti–Zr–Ni alloys which can be cast to the amorphous state using a 300-μm-thick copper mold. For the Ti–Zr–Cu system, the best glass forming alloy was found at $Ti_{35}Zr_{10}Cu_{55}$, which can be cast to the amorphous state to the thickness of 500 μm. The critical cooling rate for glass formation is estimated to be 2×10^4 K/s. In the present article we report two bulk glass forming regions in the Ti–Zr–Cu–Ni quaternary system. Here, we rather arbitrarily define a "bulk" metallic glass as having a minimum dimension of 1 mm equivalent to a critical cooling rate of 4×10^3 K/s.

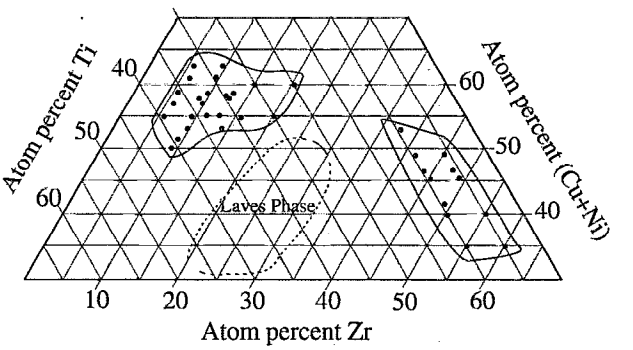

FIG. 2. Two bulk glass formation regions in the pseudoternary phase diagram. The dots represent the alloys which can be cast to amorphous strips of at least 1 mm thickness. Generally for the titanium-rich region the nickel concentration is about 4–12 at. %. The glass forming region is largest when nickel concentration is about 8 at. %. For the zirconium-rich region, copper and nickel are roughly interchangeable when at least 4 at. % of either copper or nickel is used. The region moves downward with increasing nickel concentration. In the center of the diagram the quaternary Laves phase field is shown.

II. EXPERIMENT

Ingots of alloys were prepared by induction melting 99.99% pure Ti, 99.8% pure Zr, 99.999% pure Cu, and 99.97% pure Ni on a water-cooled silver or copper boat under a Ti-gettered argon atmosphere. The nominal compositions are used in the current article. The weight loss of the samples by alloying was less than 0.1%. Thus, the compositions of the alloys did not change significantly after melting. The alloy ingots were then remelted under vacuum in a quartz tube using an rf induction coil and then injected into a copper mold under pure argon at about 1 atm pressure. The copper mold has internal strip-shaped cavities of about 2 cm length, 4–6 mm width, and varying thickness of 300 μm, 500 μm, 1 mm, 2 mm, 3 mm, and 4 mm. This yields cast samples of varying strip thickness. The typical length of the resulting strips is 20 mm. The typical dimensions of the strip cross sections are 1×4, 2×4, 3×4 or 4×6 mm^2. The crystalline/amorphous nature of the strips was determined by x-ray diffraction, using a 120° position sensitive detector (Inel) and a collimated Co $K\alpha$ x-ray source. To ensure the amorphous nature of the interior of the strips, some strips were cut longitudinally in half, and the cross-sectional surfaces were examined by x-ray diffraction. The glass transition and crystallization behavior were studied using a Perkin–Elmer differential calorimeter (DSC-4). The melting temperatures of the crystalline alloys were measured using a Setaram high-temperature differential thermal analysis (DTA). Vicker's hardness of the material was obtained using a Leitz microhardness tester.

III. RESULTS

A. Glass forming regions

Figure 2 illustrates two regions of the quaternary composition space in which bulk glass formation (>1 mm thick-

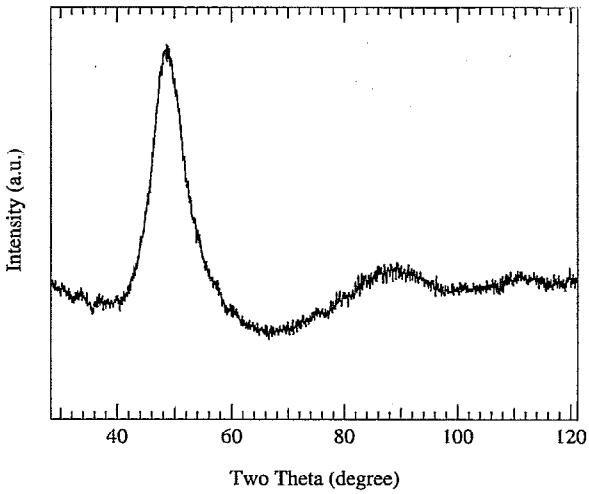

FIG. 3. X-ray-diffraction pattern (Co $K\alpha$ radiation) taken from the cross-sectioned surface of 4×6×20 mm^3 $Ti_{34}Zr_{11}Cu_{47}Ni_8$ strip obtained by metal mold casting.

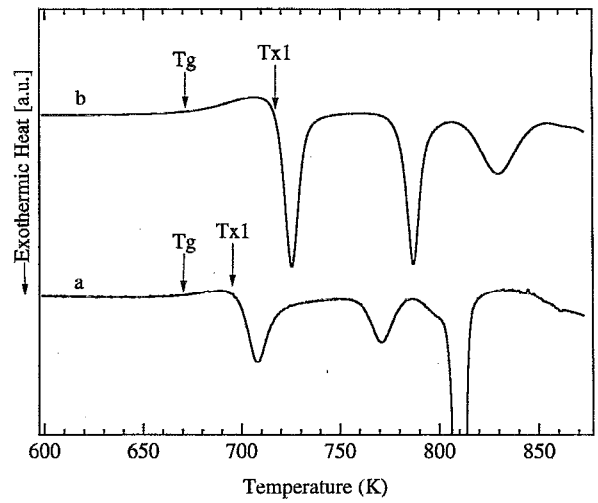

FIG. 4. DSC scans of amorphous alloys. T_g is the onset of glass transition temperature, T_{x1} is the onset of first crystallization temperature, and so on. (a) $Ti_{35}Zr_{10}Cu_{55}$. (b) $Ti_{34}Zr_{11}Cu_{47}Ni_8$.

ness) was found. Notice that the diagram is pseudoternary, the information regarding the copper/nickel ratio is not seen. Generally, for the titanium-rich region, the nickel concentration is about 4–12 at. %. The glass forming region is largest when the nickel concentration is about 8 at. %. For the zirconium-rich side, copper and nickel are interchangeable when one maintains a minimum of 4 at. % of either copper or nickel. This region tends to shift downward with increasing nickel concentration. The admixture of Cu and Ni improves the GFA tremendously. The best Ti–Zr–Cu amorphous alloy is $Ti_{35}Zr_{10}Cu_{55}$, having a maximum glass thickness or about 0.5 mm. $Ti_{34}Zr_{11}Cu_{47}Ni_8$ is the best quaternary Ti–Zr–Cu–Ni amorphous alloy. It can be cast at least 4 mm thick. The estimated critical cooling rate for glass formation of this alloy is about 250 K/s or lower. It is two orders of magnitude lower than that of the best ternary Ti–Zr–Cu glass former. We also found that when an alloy was cast to a strip thicker than its maximum thickness for glass formation, the outer layer of the strip remains amorphous, while the core is crystalline. This suggests that the glass forming ability of these alloys is restricted by homogeneous nucleation in the sample interior, rather than by heterogeneous nucleation at the copper mold interface, if we assume there are no heterogeneous nucleation sites within the molten liquid. Figure 3 shows the x-ray-diffraction pattern for one of the strips. No peaks corresponding to crystalline phases can be detected.

B. Thermal analysis of the amorphous alloys

Figure 4 shows the DSC traces of two amorphous alloys taken using a heating rate of 20 K/min. They exhibit an endothermic heat event characteristic of the glass transition followed by four characteristic exothermic heat release events indicating the successive stepwise transformations from a metastable undercooled liquid state to the equilibrium crystalline intermetallic phases at different temperatures. T_g is defined as the onset of the glass transition temperature, T_{x1} is the onset temperature of the first crystallization event, etc. ΔT, defined as $T_{x1}-T_g$, is referred to as the supercooled liquid region. For the $Ti_{34}Zr_{11}Cu_{47}Ni_8$ amorphous alloy, T_g=671 K, T_{x1}=717 K, and ΔT=46 K, respectively. For the $Ti_{35}Zr_{10}Cu_{55}$, T_g=668 K, T_{x1}=697 K, and ΔT=29 K, respectively. Table I shows glass transition and crystallization temperatures of some of the representative glass forming alloys. Figure 4 shows a high-temperature DTA scan of the crystalline alloy $Ti_{34}Zr_{11}Cu_{47}Ni_8$. The alloy begins to melt at a solidus temperature T_{sol}=1105 K followed by complete melting at the liquidus temperature T_{liq}=1160 K.

C. Mechanical properties

Vicker's hardness measurements on these amorphous strips have been carried out. The typical accuracy of the measurement is 3%. Table II shows the Vicker's hardness of some representative glassy alloys. In terms of hardness, the composition dependence Ni>Cu≫Zr>Ti is generally observed. The value for $Ti_{34}Zr_{11}Cu_{47}Ni_8$ alloy is H_v=628±20

TABLE I. Glass transition and crystallization temperatures of some representative glass forming alloys at heating rate of 20 K/min. The missing crystallization temperatures are due either to the absence of crystallization peaks up to 873 K, or to the crystallization temperature being too close to 873 K to be determined accurately. Here 873 K is the maximum working temperature of the DSC.

Composition								
Ti	Zr	Cu	Ni	T_g (K)	T_{x1} (K)	T_{2x} (K)	T_{x3} (K)	T_{x4} (K)
35	10	55	0	668	697	760	805	
33	13.4	49.6	4	674	694	758	800	
34	11	47	8	671	717	778	813	
33.4	11.9	42.7	12	671	724	780		
9.9	43.3	42.8	4	657	691	742	791	
9.5	45.2	37.3	8	653	690	729	769	
9.5	48.9	29.6	12	637	678	709	748	782
10	50	20	20	644	680	749	759	780

TABLE II. Vicker's hardness of some representing glass forming alloys determined using a load of 500 g.

Composition				
Ti	Zr	Cu	Ni	H_v (kg/mm^2)
36.9	5.8	53.3	4	562
33	5.8	57.2	4	626
33	9.6	53.4	4	618
34	11	47	8	628
39.6	5.5	46.9	8	596
35.9	5.5	50.6	8	616
32.2	5.5	54.3	8	642
28.5	9.2	54.3	8	670
32.2	9.2	50.6	8	618
28.5	12.9	50.6	8	626
9.5	37.8	44.7	8	616
9.5	41.5	41	8	553
9.5	45.2	37.3	8	519
9.5	48.9	33.6	8	501
10	55	25	10	462
5.8	45.2	41	8	536
5.8	48.9	37.3	8	523
5	55	32	8	487
10	50	20	20	499
10	50	15	25	558

kg/mm^2. Using the well-known relation $H_v = 3\sigma_y$,[14] the yield strength of this amorphous alloy is estimated to be around 2 GPa.

One 2-mm-thick $Ti_{34}Zr_{11}Cu_{47}Ni_8$ amorphous strip was successively rolled at room temperature using a thickness reduction of 1.5% deformation per step down to a 0.15-mm-thick ribbon without cracking. This demonstrates the ductile behavior of the amorphous material when deformation occurs under a confined geometry. The resulting ribbon can be further bent 180° without failure. The Vicker's hardness of the resulting ribbon was also measured and agrees with that of the initial strip within the experiment accuracy. This indicates that there is no work hardening as is expected for an amorphous material.

IV. DISCUSSION

In Fig. 1, we see a strong T_{rg} dependence of the glass forming ability of metallic alloys. High values of T_{rg} are associated with good glass forming ability. For example, $Pd_{40}Ni_{40}P_{20}$ alloy has $T_{rg}=0.66$,[3,15] $Au_{55}Pb_{22.5}Sb_{22.5}$ alloys have $T_{rg}=0.63$.[6] Their critical cooling rates are 10^3 K/s or less. The recently found $Zr_{41.2}Ti_{13.8}Cu_{12.5}Ni_{10}Be_{22.5}$ alloys have $T_{rg}=0.67$,[4] and have critical cooling rate of 1 K/s.[5] The T_{rg} of $Ti_{34}Zr_{11}Cu_{47}Ni_8$ is 0.578, by comparison not a very high value. According to Fig. 1, the estimated critical cooling rate for an alloy of $T_{rg}=0.578$ would typically be of the order of 10^5 K/s. Therefore, from the point of view of reduced glass transition temperature, the GFA of Ti–Cu–Zr–Ni alloys such as $Ti_{34}Zr_{11}Cu_{47}Ni_8$ is relatively better than expected (see Fig. 5). In fact, this is not unique. Some newly found multicomponent alloys, such as $Mg_{65}Cu_{25}Y_{10}$ (Ref. 8) and $Zr_{65}Cu_{17.5}Ni_{10}Al_{7.5}$ (Ref. 9) also show better GFA than expected from T_{rg}. Three factors, a significantly different atomic size among the constituent elements, a large negative heat of mixing, and the necessity of substantial redistribution of the component elements for the progress of crystallization, have been cited and used to interpret the unexpected good GFA of these systems.[16] In fact, the first two factors, large atomic size ratios and large negative heat of mixing, are already reflected by the relatively low lying eutectic melting temperatures of these alloys. As such, these factors give, at best, a qualitative glass forming criteria, whose role is not quantified. In conventional homogeneous nucleation theory, one evaluates GFA by considering the competition between a decreasing nucleation barrier and an increasing viscosity with increasing undercooling of the liquid. If the nucleation crystalline phase has a composition very different from that of the undercooled liquid, only when the composition of a local liquid region the size of a critical crystalline nucleus satisfies the composition requirements of the crystalline phase (either by fluctuation of liquid decomposition) can crystallization occur. For higher-order multicomponent systems, it is more difficult for the concentrations of all elements to simultaneously satisfy the composition requirements of crystalline phase than for lower-order systems. As such, the crystallization process of the multicomponent undercooled liquid will tend to be more sluggish than for simpler systems. The multicomponent alloys may thus exhibit better GFA than predicted from the point of view of the reduced glass transition temperature alone. The fundamental argument used here has been loosely called the "confusion principle."[17] The concept is that as the number of components in a liquid alloy is increased, crystallization becomes confused or frustrated. Recently, Desre has quantified this argument.[18] He considered a multicomponent system with n equally concentrated component elements. For $n=2$ to $n=10$, the addition of each additional component to the alloy is predicted to lower by an order of magnitude the probability of the concentration fluctuation within a cluster of 600 atoms for crystallization. The probability of achieving a critical nucleus of the required composition is lowered by an order of magnitude with the addition of each new compo-

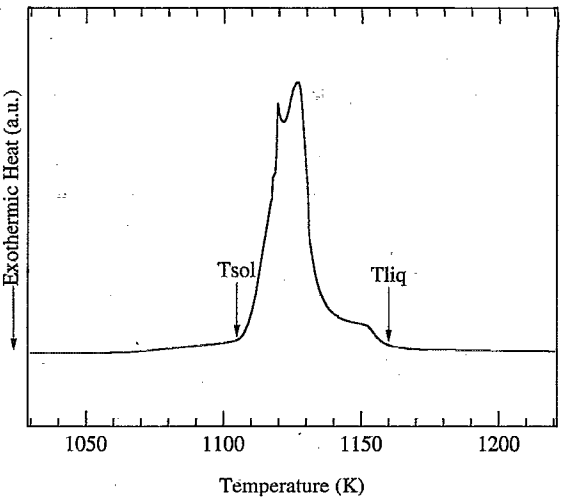

FIG. 5. High-temperature DTA scan of $Ti_{34}Zr_{11}Cu_{47}Ni_8$. T_{sol} is the solidus temperature, T_{liq} is the liquidus temperature.

nent. Thus, the more complex the alloy, the better the GFA. This argument may explain the extraordinary good GFA of the present Ti–Zr–Cu–Ni system and the Zr–Cu–Ni–Al (Ref. 9) and Mg–Cu–Y (Ref. 8) systems as well. One piece of evidence in support of this argument is that all good glass forming alloys in these systems show a large undercooled liquid region, as indicated by the temperature interval between glass transition and first crystallization event during sample heating. The nucleation of crystalline phases from the undercooled liquid phases requires substantial atomic diffusion and composition redistribution. In this situation, the undercooled liquid is relative stable against the crystallization. Note that for the $Ti_{34}Zr_{11}Cu_{47}Ni_8$ amorphous alloy $\Delta T=46$ K, while for the $Ti_{35}Zr_{10}Cu_{55}$ alloy $\Delta T=29$ K. ΔT correlates with the relative GFA of these two alloys.

It is noteworthy that a large number of early transition-metal/late-transition-metal systems exhibit the $MgZn_2$ or the $MgCu_2$-type Laves phases. Examples are: $TiMn_2$, $ZrMn_2$, $TiFe_2$, and $TiZn_2$ (of $MgZn_2$-type structure), and $ZrFe_2$, $ZrCo_2$, and $ZrZn_2$ (of $MgCu_2$-type structure). The congruent melting temperatures of these Laves phases are generally above 1600 K and the liquidus curves are relatively flat (with respect to composition). The Laves phase homogeneity ranges are often as large as 10 at. % or more.[11] These factors suggest that the Gibbs free-energy function of the Laves phases varies slowly with composition. In this sense, the Laves phases are somewhat similar to liquid or glassy phase. They are both "forgiving" of composition variation. On the other hand, there are no equilibrium binary Ti–Cu, Ti–Ni, Zr–Cu, or Zr–Ni Laves phases. The melting temperature of Ti_2Ni is lowered by adding Zr, and the melting temperature of Zr_2Ni is lowered by adding Ti. One would expect an extremely low lying liquidus temperature in the center of the Ti_2Ni–Zr_2Ni section if there were no ternary Laves phase. In the actual ternary Ti–Ni–Zr system, the Laves phase enters the diagram with a homogeneity range from 21 to 30 at. % Zr at 970 K.[10] One expects similarly large homogeneity ranges for the ternary Ti–Cu–Zr Laves phase as well as the quaternary Ti–Zr–Cu–Ni Laves phase. Because of the relative insensitivity of the Laves phase to composition variations, it may nucleate more easily than the other competing crystalline phases from the undercooled liquid. We have determined that there are two quaternary eutectics near the compositions of $Ti_{37}Zr_{17}Cu_{42}Ni_4$ and $Ti_{17}Zr_{40}Cu_{28}Ni_{15}$, respectively. Interestingly, these two alloys cannot be cast to 0.5-mm-thick amorphous strips. By comparison, $Ti_{34}Zr_{11}Cu_{47}Ni_8$ can be cast to 4-mm-thick amorphous strips and $Ti_{10}Zr_{49}Cu_{33}Ni_8$ can be cast to at least 2-mm-thick amorphous strips. Their reduced glass transition temperatures are in fact lower than those of the two eutectic alloys, but their critical cooling rates for glass formation are at least one and possibly two orders of magnitude lower than those of the two eutectic alloys. They are much better glass formers. We suggest that this is due to the compositions being relatively far from that of the Laves phase. To obtain a good glass forming composition in Ti–Zr–Cu–Ni system, one must consider two factors: First, one should be close to the eutectic points to obtain a high reduced glass transition temperature; second, one must avoid the Laves phase which apparently nucleates relatively more easily than other competing crystalline phases. The best glass forming alloys of the present Ti–Zr–Cu–Ni system are examples of simultaneously satisfying these two conditions.

The main obstacle which prevents us from getting better GFA in the Ti–Zr–Cu–Ni system is the existence of the quaternary Laves phase. To improve the GFA of the Ti–Zr–Cu–Ni system, one must find a way to eliminate or at least destabilize the Laves phase to achieve a lower melting temperature alloy in the center of the quasiternary phase diagram. We have found that transition metals having a high melting temperature Laves phase with Ti or Zr tend to stabilize the Laves phase of the quaternary alloy and thus degrade the GFA. On the other hand, substituting Cu or Ni by Zn or Co does not degrade the glass forming ability. If the fifth element added is metalloid element such as B or Si, the alloy loses its GFA. In this case, crystallization is apparently triggered by the precipitation of very stable Ti or Zr borides or silicides. It seems the only way to improve the glass forming ability of current Ti–Zr–Cu–Ni system is to add Be as has already been proven.[4,5] Apparently the very small atomic radius of Be is incompatible with the preferred atomic size ratio of the Laves phase. As such, Be acts to destabilize the quaternary Laves phase resulting in further depression of the alloy liquidus curve in the center portion of the quaternary alloy diagram. This yields a pentiary alloy with a eutectic at 943 K[2]. From this point of view, we can understand why the Zr–Ti–Cu–Ni–Be system is such an exceptional glass former.

From the above arguments, one concludes that while the reduced glass transition temperature still plays a dominant role in determining the GFA of metallic alloys, the requirement that the crystallization involve large composition fluctuations in the liquid phase also tends to enhance the GFA tremendously.

V. CONCLUSIONS

Bulk metallic glass formation in the ternary Ti–Zr–Cu–Ni system is reported. Bulk samples of metallic glass can be prepared by metal mold casting up to dimensions of several millimeters. The critical cooling rate for glass formation is of the order of 500 K/s. For the particular amorphous alloy $Ti_{34}Zr_{11}Cu_{47}Ni_8$, the hardness is about 628 kg/mm^2, while the tensile strength is estimated to be about 2 GPa. Comparing with the Zr–Ti–Cu–Ni–Be system, the quaternary alloys have relatively poorer GFA. On the other hand, the absence of Be in these glasses may make them of interest from the point of view of applications.

It has been noted that the GFA of the quaternary alloys is better than might be expected based on their reduced glass transition temperature alone. This suggests that the requirement for composition fluctuations and diffusion controlled nucleation play an important role in determining the GFA of alloys.

The greatly enhanced GFA obtained by adding a few percent of a fourth element in the present alloy system suggests that making a system more complex is a practical way to search for new bulk glass forming alloy systems.

ACKNOWLEDGMENTS

The authors would like to thank N. Zhang for preparing some of the specimens. The financial support from the Department of Energy (Grant No. DE-FG03-86ER45242) is greatly acknowledged.

[1] D. Turnbull, *Solid State Physics* (Academic, New York, 1956), Vol. 3, p. 225.
[2] F. Spaepen and D. Turnbull, in *Rapid Quenched Metals*, edited by N. J. Grant and B. C. Giessen (MIT Press, Cambridge, MA, 1976), p. 205.
[3] H. A. Davies, in *Rapidly Quenched Metals III*, edited by B. Cantor (Metals Society, London, 1978), Vol. 1, p. 1.
[4] A. Peker and W. L. Johnson, Appl. Phys. Lett. **63**, 2342 (1993).
[5] Y. J. Kim, R. Busch, W. L. Johnson, A. J. Rulison, and W. K. Rhim, Appl. Phys. Lett. **65**, 2136 (1994).
[6] M. C. Lee, J. M. Kendall, and W. L. Johnson, Appl. Phys. Lett. **40**, 382 (1982).
[7] A. Inoue, T. Nakamura, T. Sugita, T. Zhang, and T. Masumoto, Mater. Trans. JIM **34**, 351 (1993).
[8] A. Inoue, A. Kato, T. Zhang, S. G. Kim, and T. Masumoto, Mater. Trans. JIM **32**, 609 (1990).
[9] A. Inoue, T. Zhang, N. Nishiyama, K. Ohba, and T. Masumoto, Mater. Trans. JIM **34**, 1234 (1993).
[10] V. V. Molokanov, V. N. Chebotnikov, and Yu. K. Kovneristyi, Inorg. Mater. **25**, 46 (1989).
[11] *Binary Alloy Phase Diagrams*, 2nd ed., edited by T. B. Massalski (ASM International, Metals Park, OH, 1990).
[12] C. G. Woychik and T. B. Massalski, Z. Metal. **79**, 149 (1988).
[13] T. B. Massalski, C. G. Woychik, and J. Dutkiewicz, Metal. Trans. A **19**, 1853 (1988).
[14] L. A. Davis, in *Mechanical Behavior of Rapidly Solidified Materials*, edited by S. M. L. Sastry and B. A. MacDonald (The Metallurgical Society, Inc., Warrendale, PA, 1986).
[15] A. J. Drehman and A. L. Greer, Acta Metall. **32**, 323 (1984).
[16] A. Inoue, T. Zhang, and T. Masumoto, J. Non-Cryst. Solids **156-158**, 473 (1993).
[17] A. L. Greer, Nature **366**, 303 (1993).
[18] P. J. Desre, Mater. Forum (to be published).